

# Quark degrees of freedom in nuclear matter

**Marcello Baldo**

Istituto Nazionale di Fisica Nucleare, Sez. Catania, via S. Sofia 64, 95123 Catania (I)

E-mail: [baldo@ct.infn.it](mailto:baldo@ct.infn.it)

**Abstract.** The microscopic theory of Nuclear Matter has been approached along the years by different many-body methods and different nucleon-nucleon (NN) interactions. The realistic NN interactions can be classified mainly into two categories. One relies on the meson-nucleon coupling scheme, within relativistic or non-relativistic framework. The so-called chiral interactions are based on the assumption that, once the pion exchange contribution has been explicitly isolated, it is possible to expand the NN interaction in a series of point interaction terms which respect the underlying QCD chiral symmetry. In both schemes three-body (TBF) or higher forces can be constructed, which can have different degrees of phenomenological character. The TBF are essential to get the Nuclear Matter saturation point close to the phenomenological one. However the QCD quark degrees of freedom are not explicitly introduced. It will be shown that a realistic NN interaction that is constructed from the quark degrees of freedom can produce the correct saturation point without the need of TBF. The corresponding Equation of State is compatible with all the phenomenological constraints, including the Neutron Star maximum mass limit. Taking this result literally, one can say that quarks have been revealed in Nuclear Matter. Another conclusion is that the effect of TBF is model dependent.

## 1. Introduction

The Equation of State of Nuclear Matter is of great relevance for numerous area of physics and the corresponding phenomena [1]. It is essential for the physics of heavy ion (HI) reactions at intermediate energies, supernovae (SN) and Neutron Stars (NS) and gravitational wave (GW) emission from binary mergers or NS oscillations. The physical conditions of nuclear matter is quite different in each one of these systems. In HI matter can be compressed at few times saturation density, it is close to be symmetric and the temperature is relatively low with respect to the Fermi energy. In SN matter is strongly asymmetric, it is present in a very wide density range, from vanishing small values to about twice saturation density, and the temperature can be as high as several tens of MeV. In NS the matter is mainly cold, very asymmetric and compressed up to several times saturation density. Finally in GW emission the asymmetry is large, the temperature is close to the one for SN and the density is always close to the maximum one obtainable without collapse to a black hole.

These phenomena can be analyzed in a more or less model dependent methods, but in any case they provide severe constraints on the EoS. Within a phenomenological approach, e.g. on the basis of effective mean fields models, these constraints do not fix tightly the EoS, which therefore cannot be accurately known. Alternatively one can try to develop a microscopic many-body theory of nuclear matter and check to what extent they are compatible with the phenomenological constraints. The comparison among different theoretical methods can provide an estimate of the theoretical uncertainty on the EoS and the comparison with



the phenomenological constraints can eventually rule out some of the microscopic EoS. We will show that most of the microscopically derived EoS are compatible with the phenomenological constraints developed up to now, which implies that the microscopic structure of nuclear matter, as predicted by the different theoretical models, is not well constrained. In particular the presence and strength of three-body force (TBF) turns out to be dependent on the nucleon-nucleon (NN) interaction models. Furthermore if the quark degrees of freedom are explicitly introduced in the NN interaction model, the role of TBF seems to be strongly reduced. This shows the relevance of introducing explicitly the effective quark degrees of freedom.

An analysis of the future experiments and of the possible observations shows how they are expected to select severely among the different EoS.

## 2. Overview of the microscopic methods

A microscopic many-body method is characterized mainly by two basic elements, the realistic bare interaction among nucleons and the many-body scheme followed in the calculation of the EoS. There are three basic classes of bare nucleonic interactions

- Interactions mediated by meson exchanges
- Chiral expansion approach
- Models that include explicitly the quark-gluon degrees of freedom

The many-body methods can be enumerated as follows

- The Bethe-Brueckner-Goldstone (BBG) diagrammatic method and the corresponding hole-line expansion
- The Coupled Cluster (CC) expansion
- The relativistic Dirac-Brueckner (DBHF) approach
- The self-consistent Green's function (SCGF)
- The variational method
- The renormalization group (RG) method
- Different methods based on Monte-Carlo (MC) techniques

We will proceed along the list of the nucleonic interactions, and for each class the results with different many-body methods that have been employed will be discussed. The simplest constraint that has to be considered is the reproduction of the phenomenological saturation point, and we will see to what extent this condition is fulfilled. Later other constraints will be discussed.

The Argonne v18 [2] potential is a meson exchange potential that was widely used in the calculation of the EoS with different many-body methods. The meson degrees of freedom in this case are not explicitly introduced, but the form factor of the series of operators which define the potential are mainly suggested by the static limit of meson exchange processes. The parametrization of these form factors results in an excellent fit of the available NN phase shifts and deuteron data. The result of the BBG calculation of the EoS for symmetric matter using this interaction is reported in Fig. 1, taken from ref. [3]. Here the full lines correspond to the calculations including only two-body correlations, i.e. at the Brueckner-Hartree-Fock level. The two full lines correspond to two different choices of the effective single particle potential, the so-called gap choice and continuous choice. In the former the single particle potential is set to zero above the Fermi energy, while in the latter it is calculated for all relevant momenta. One can see that there is some discrepancy. However when the three-body correlations are included, corresponding to the three-body cluster contribution, the final EoS look quite close to each other (square and circle symbols). This indicates a convergence of the BBG expansion, since if all the diagrammatic contributions, corresponding to the hole-line expansion, would be added, the result must be independent on the single particle potential. The latter is just an

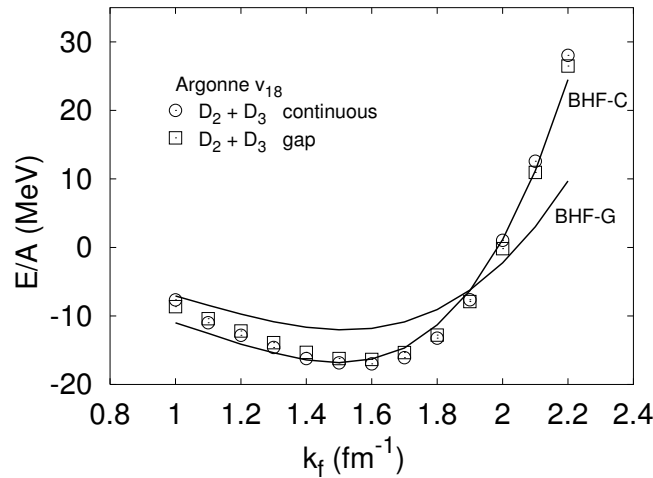


**Figure 1.** EoS for the NN interaction  $Av_{18}$  within the BBG expansion. The two full lines correspond to the calculations at the two hole-line level of approximation (Brueckner-Hartree-Fock) with the gap choice (BHF-G) and with continuous choice (BHF-C), respectively, for the auxiliary single particle potential. The symbols correspond to the EoS when the three hole-line contributions are included. Figure taken from ref. [3]

auxiliary quantity, useful to speed up the rate of convergence of the expansion. However one can see that the saturation point is not reproduced, since it can be nominally taken at energy per particle  $E/A = -16$  MeV and  $k_F = 1.33 \text{ fm}^{-1}$ , with some uncertainty, much smaller than the discrepancy. This result is systematic for all the meson exchange potential, independently of the many-body method employed. This calls for the introduction of three-body forces (TBF). This can be performed at phenomenological level or by evaluating again the processes involving three nucleons in an irreducible way [4]. In Fig. 2, taken from ref. [5], are reported the EoS calculated with phenomenological TBF within the BBG scheme (squares) and the variational method (circles). The TBF were adjusted to reproduce the saturation point, by varying mainly one parameter. The agreement is somehow misleading since the EoS from variational method has been modified with an additional correction by hand around saturation, which turns out to be of about 3 MeV at saturation density. The agreement at higher density is a genuine one. The effect of TBF is quite moderate around saturation but they are essential to get the correct saturation point.

Two-body forces based on meson exchange model can be used in a relativistic framework. One can try to formulate the BHF equations, in particular the one for the G-matrix, within a relativistic formalism. This is a difficult task, and in general one keeps the interaction as instantaneous (static limit) and a reduction to a three-dimensional formulation from a four-dimensional one. This is the Dirac-Brueckner scheme, where the main relativistic effect is due to the use of the spinor formalism. It turns out that the relativistic formulation produces a saturation effect, and one can get the correct saturation point by a suitable realistic NN interaction [6]. It has been shown [7] that the use of spinors has the effect of introducing a particular TBF, if they are projected into the bare particle states. In fact the presence of the single particle potential in the the so-called small components of the spinors produces a "rotation" of the spinors with respect to the free ones, which results in the appearance of anti-particle states. At non relativistic level this is equivalent to the effect of a TBF where a particle-antiparticle pair is created in the intermediate state [7], the so-called Z-diagram. However at the non-relativistic level other TBF can be present, and it is unclear if they would affect these

results at relativistic level.

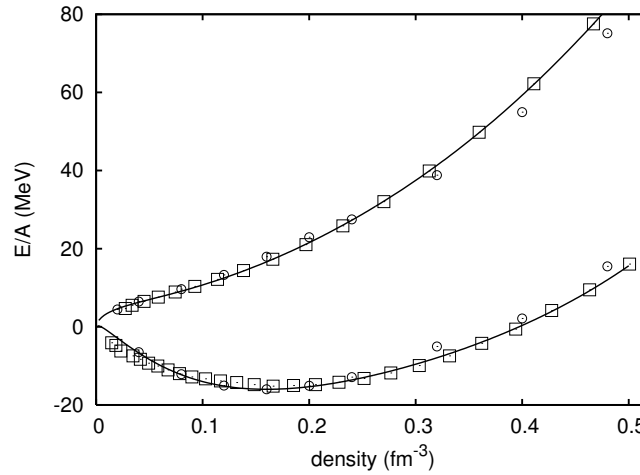


**Figure 2.** EoS for the NN interaction Av18 plus phenomenological three-body forces, for pure neutron matter (upper part) and symmetric matter (lower part). The squares correspond to the BHF calculation [5], the circles to the variational one of ref. [8]. The full lines correspond to a polynomial fit to the BHF calculation. Figure taken from ref. [5].

An approach more closely related to the underlying QCD structure of nucleons is the chiral scheme, originally devised by Weinberg [9]. In this case one includes in the interaction a series of operators which reflect the partially broken chiral symmetry of QCD. To this purpose a non-linear representation of the  $SU(2) \times SU(2)$  chiral group is introduced and the form of the operators invariant with respect to the representation is then fixed. The strength parameters associated to each operator are then determined by fitting the NN phase shifts, the properties of deuteron and eventually of few-body nuclear systems. The method is then implemented in the framework of the Effective Field Theory (EFT), i.e. by ordering the terms according their dependence on the physical parameter  $Q/M$ , where  $M$  is the nucleon mass and  $Q$  a generic momentum that appears in the Feynman diagram for the considered process. This parameter is assumed to be small. Each term is dependent on a given power of this parameter and therefore this fixes its relevance. In this way a hierarchy of the different terms of the forces is established. In particular one finds that the three-body forces so introduced are of higher order than the simplest two-body forces. In practice this procedure amounts to expand the nuclear force in a series of point interactions with possible derivatives, except for the pion degrees of freedom that are treated separately and with the proper range. In comparison with the meson exchange model this is equivalent to treat the pion as an explicit degree of freedom, while the exchange of heavier meson is expanded in the transfer momenta. This is illustrated in Figs. (3,4), where some two-body and three-body forces respectively are depicted. The dashed lines indicate pion propagation, a full dot a derivative coupling. The assumption of a small  $Q/M$  parameter in principle restricts the applications of these forces to not too large momenta and therefore to a not too large density of nuclear matter. It turns out that the safe maximum density is around the saturation value. This power counting has been refined along the years and many applications can be found in the literature. We restrict the discussion on few calculations that illustrate the different approaches to the nuclear matter EoS.

One of the main characteristics common to these forces is the critical relevance of the TBF in the saturation mechanism. In fact, as illustrated in Fig. 5, taken from ref. [10], without TBF the EoS does not display an apparent saturation, and anyhow close to saturation density the TBF

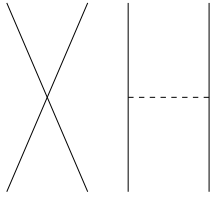


**Figure 3.** Chiral two-body forces. The full lines indicate nucleon propagation, the dashed lines indicate pion propagation, which results in a finite range interaction. A simple crossing between two nucleon lines indicates a point interaction, and a full dot correspond to a derivative coupling.

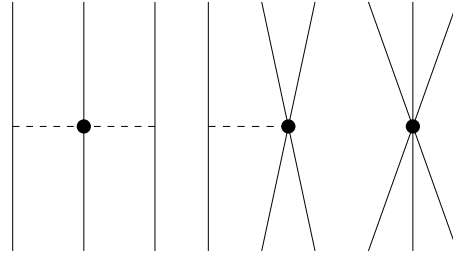


**Figure 4.** Chiral three-body forces. The meaning of the symbols is the same as in Fig. 3

contribution is quite large, of several MeV, in contrast to the case of meson exchange interactions, where the TBF contribution around saturation is of the order of 1 MeV. These calculations are perturbative in character, as indicated in the labels, but this feature holds true also in more refined calculations. Notice the relevance of the momentum cutoff, that is introduced in order to control the point interaction forces, that otherwise would produce a divergent contribution. In general the chiral two-body forces are evolved according the Renormalization Group (RG) method before they are employed in the many-body calculations, like in ref. [10]. The same procedure has been followed in the BHF calculations of ref. [11], where a similar relevance of the TBF was found. The most sophisticated many-body calculations with chiral forces is probably the ones of ref. [12], where the CC method was employed up to a selected set of three-body clusters. In this paper it was also found that it is difficult with the same chiral forces to fit both the binding of few nucleon systems (  $H$ ,  $^3He$  ) and the saturation point. This feature is common to the meson exchange forces discussed above, for which the same difficulty was found. A similar conclusion was found in the BHF calculations of ref. [13], where it is suggested to fit simultaneously the few-body binding and the saturation point.

Another approach inspired by the QCD theory of strong interaction has been developed by a few groups [14, 15, 16, 17, 18, 19, 20]. In this approach the quark degree of freedom is explicitly introduced and the nucleon-nucleon interaction is constructed from gluon and meson exchange between quarks, the latter being confined inside the nucleons. One of these quark models (QMS) of the nucleon-nucleon interaction, named fss2 [20, 21], is able to reproduce closely the experimental phase shifts and the few-body binding energies [21, 22, 23, 24]. In particular triton binding energy is reproduced within 300 KeV. More recently it has been shown [25] that the fss2 interaction is able to reproduce also the correct nuclear matter saturation point without any additional parameter or need to introduce TBF. This is illustrated in Fig. 6, taken from ref. [25], where the EoS for symmetric matter is reported. The scheme of this figure follows

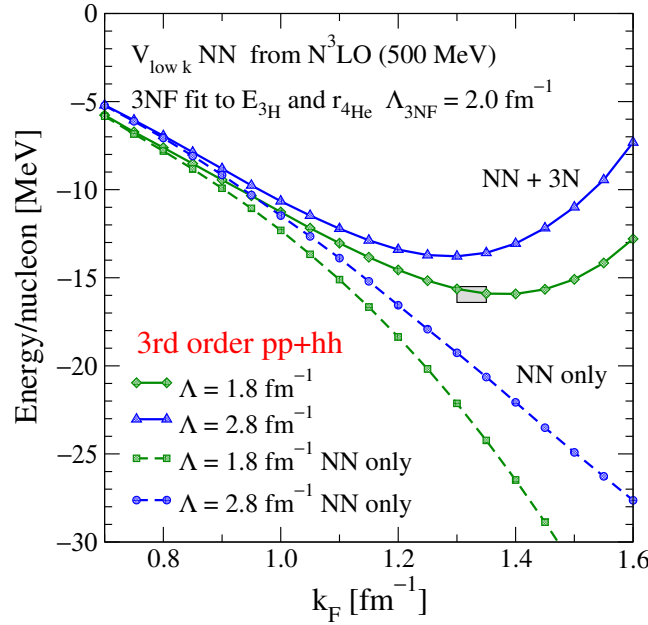


**Figure 5.** EoS of symmetric nuclear matter including third order perturbative corrections based on chiral interaction at  $N^3\text{LO}$  level. The cutoff for three-body forces is fixed at  $\Lambda_{3N} = 2.0 \text{ fm}^{-1}$ , while the cut-off  $\Lambda$  of the (evolved) chiral two-body interaction is set equal to the two indicated values. Figure taken from ref. [10].

the one of Fig. 1. The open symbols correspond to the EoS calculated at the BHF level of approximation with the gap and the continuous choices, while the full symbols correspond to the EoS calculated by including the three hole-line contribution. One can see that also in this case the final EoS is insensitive to the choice of the single particle potential. However in this case the three hole line contribution is minimal for the gap choice.

The main result of this calculation is that the saturation point is reproduced without the introduction of three-body forces.

Notice that this is the only two-body interaction that is able to reproduce with a fair accuracy both the binding of few nucleon systems and the saturation point of nuclear matter, without the need of three-body forces. The remaining small discrepancy for the few nucleon systems can be due to a (small) contribution of TBF or higher and relativistic effects.

The conclusion one can draw from this rapid review of results with different forces is that the relevance of TBF is model dependent and that the explicit introduction of the quark degrees of freedom reduce strongly the relevance of the TBF and allows to connect few-body systems to nuclear matter.

### 3. Phenomenological tests of the different EoS.

Several phenomenological constraints on the nuclear matter EoS have been devised along the years. They are discussed in few review papers [26, 1, 27]. Here we present a discussion on the comparison of different EoS with these phenomenological constraints with the purpose of possibly selecting the EoS which better respect the boundaries. We limit the analysis to the EoS that were derived from a microscopic many-body theory.

The first simple constraint is the saturation point, which is known to a certain accuracy. If we assume that the saturation density  $\rho_0$  must be in the range  $0.15 < \rho_0 < 0.17 \text{ fm}^{-3}$ , and

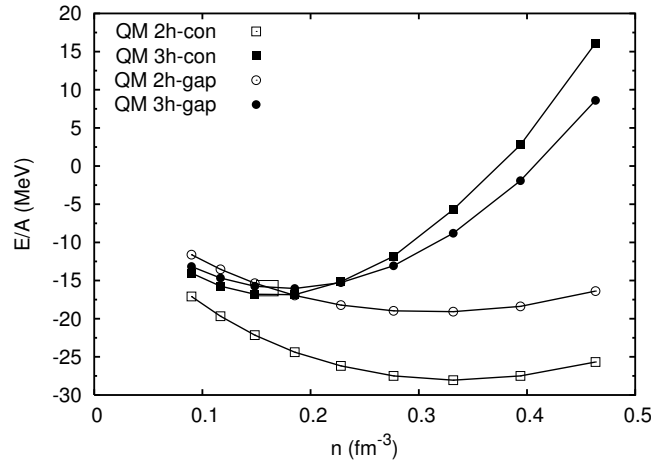


**Figure 6.** EoS of symmetric nuclear matter from the quark model interaction fss2. The open and full symbols correspond to the two hole line and three hole-line calculations, respectively. The circles and the squares indicate the calculation with the gap and continuous choices for the single particle potential, respectively. Figure taken from ref. [25]

the corresponding energy per particle  $E/A$  in the range  $-17 < E/A < -15\text{MeV}$ , then already several EoS must be ruled out. We are therefore going to mention only a set of EoS which satisfy this saturation point constraint.

A comparison among different EoS, obtained with different interactions and many-body methods, along the lines of Sec. 2, is reported in Fig. 7, taken from ref. [28], for both symmetric matter (SM) and pure neutron matter (PN).

The considered set of EoS includes variational calculations (APR) [8], BHF calculations with TBF, both phenomenological [5] and microscopically derived [4], and relativistic Dirac-Brueckner calculations [29]. The EoS from the QM interaction (FSS2), described in Sec. 2, appears to be among the softest ones in the set.

Once the energy per particle is known as a function of density, by differentiation one gets the pressure as a function of density. This allows to confront the EoS with the results of the analysis on the flow data in heavy ion reactions of ref. [30] and the ones on kaon production of ref. [31]. Such a comparison is shown in Fig. 8, taken from ref. [28], for the considered set of EoS. One can see that most of the EoS fall inside the constraint region, and the only marginal deviations occur at the highest density where the analysis is less reliable due to the onset of particle production. Again the EoS from the QM interaction looks a soft one, with respect to the others, at least at the higher density. In any case there is a fair agreement among the considered EoS and with the phenomenological boundary, a result which cannot be considered trivial or obvious. It is also clear that a refinement of the boundary could in principle put a more stringent constraint on the microscopic EoS, or even to rule out some of the EoS.

One of the main physical quantity that characterizes a given EoS is the symmetry energy as a function of the density. In ref. [32] the symmetry energy up to saturation density has been constrained from a study of the Isotopic Analog States (IAS) and the neutron skin size in neutron rich nuclei. Both of them are sensitive to the density dependence of the symmetry energy. These constraints are reported in Fig. 9. The largest box comes from the IAS analysis, while the smaller one is obtained by adding the analysis of the skin size obtained from pionic atoms and polarized hadron scattering. As a comparison the symmetry energy extracted from the EoS of the previous set is also reported. The symmetry energy from the effective interaction method



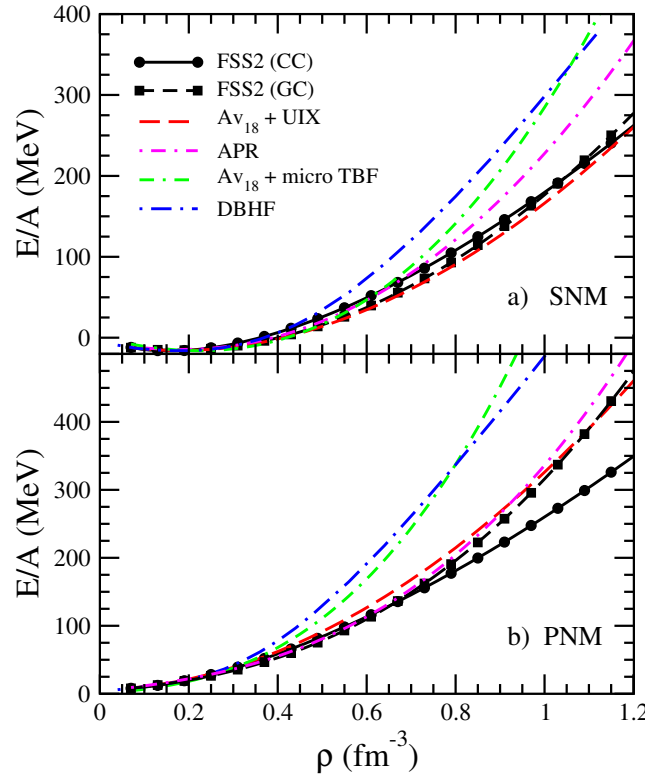


**Figure 7.** Comparison among the EoS obtained by different forces and different many-body methods. For the meaning of the labels see the text. Figure taken from ref. [28].

[33] is also reported. One can notice also in this case a fair agreement with the phenomenological constraints. Despite the shape of the symmetry energy as a function of density can be different for different EoS, the microscopic calculations fall approximately inside the allowed region. This means that the constraints cannot be used to extract a simple functional parametrization of the symmetry energy density dependence. In particular, if one assume a power law dependence, i.e.  $E_{sym} \approx \rho^\alpha$ , the exponential index  $\alpha$  cannot be constrained within a meaningful accuracy. It means also that the constraints are not appreciably selective among the microscopic EoS. In principle the BHF calculation based on  $Av_{18}$  interaction plus phenomenological TBF, the BBG calculation based on the QM interaction and the EoS from chiral forces look well inside both boundary regions of the constraints.

The extension of these calculations beyond the saturation density reveals that the agreements among the different EoS is lost. This is illustrated in Fig. 10, where one can see that the different predictions are divergent. A phenomenological constraints in this density range is likely to be strongly selective on the EoS. Unfortunately there is no stringent enough constraints at above saturation density, but it can be expected that in the relatively near future such constraints will be possibly formulated, e.g. from the planned CBM experiment [34] at FAIR. The EoS calculated with the QM interaction displays a soft dependence of the symmetry energy at high density.

As a further phenomenological constraint we consider the largest Neutron Star (NS) mass observed up to now. This is a particularly relevant constraint since it is based on direct observations, without the use of numerical simulations. Although the analysis of the data needs models for the NS atmosphere, they can be considered reliable enough to draw firm conclusions.



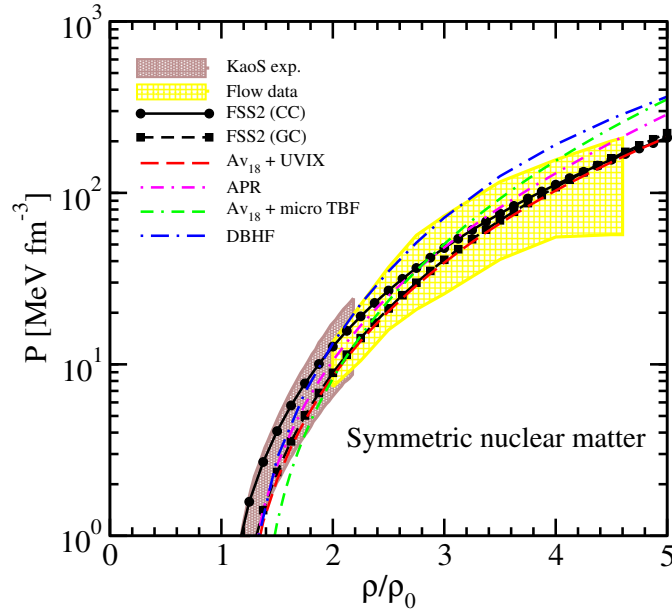


**Figure 8.** (Color online) The pressure of symmetric matter for several EoS. The larger (yellow) and smaller (violet) bands represent the phenomenological constraints from experimental data. See text for details. Figure taken from [28].

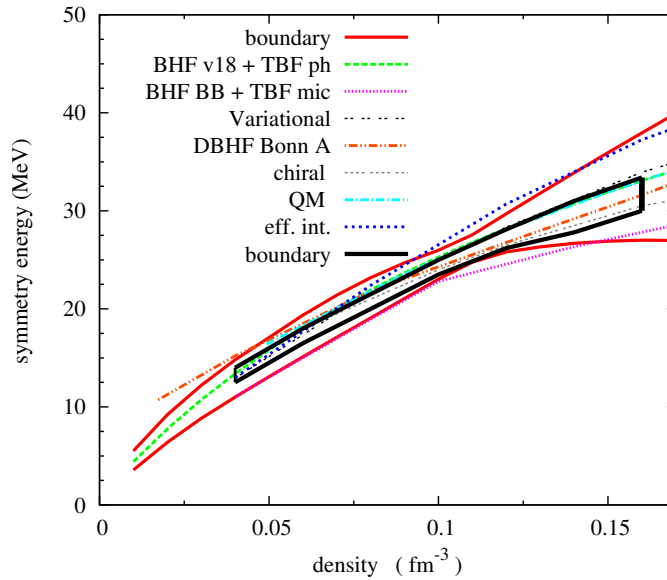


**Figure 9.** Symmetry energy as a function of density calculated with different microscopic many-body methods. The larger (red) box indicates the constraints from the analysis of the Isobaric Analog States of ref. [32]. The smaller (black) box is the boundary obtained in the same reference by adding the constraints from the neutron skin data. Figure taken from ref. [27]

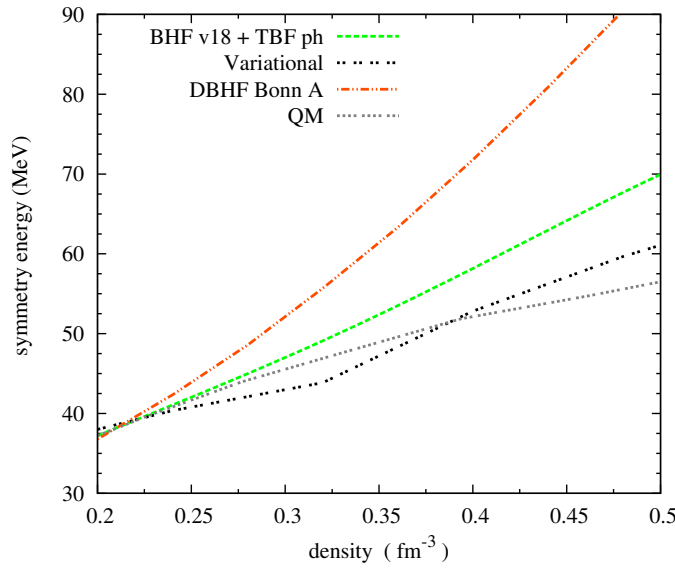


**Figure 10.** The symmetry energy above saturation density calculated with the different EoS included in Fig. 9, with exception of the EoS from the chiral approach. Figure taken from Ref. [27].

The largest mass is close to 2 solar masses [35], and in Fig. 11, taken from ref. [28] is reported the mass vs. radius and mass vs. central density relationship for NS calculated for the different EoS. These calculations employ the EoS for strongly asymmetric nuclear matter and are assuming that only nucleonic and leptonic (electrons and muons) components are present inside NS, and therefore they are sensitive also to the symmetry energy. In both panels the plots display a maximum, which is the maximum mass predicted by the corresponding EoS. This must be equal or larger than 2 solar masses if the EoS can be acceptable. The microscopic EoS which are included in this analysis seem to be compatible with observations, taking into account the uncertainty of the data [35]. For the EoS derived from QM the calculation has been performed both with the continuous choice (CC) and the gap choice (GC), and the difference between the two results can be taken as an estimate of the uncertainty of the theoretical prediction. Although the EoS in the CG and CC cases are quite close around saturation, at very high density, typical of the NS interior, they have a different incompressibility, with the EoS in the GC case slightly stiffer.

Microscopic calculations that include also the hyperon degrees of freedom, as reported in e.g. ref. [28], show that the NS matter EoS become softer, and the value of the NS maximum mass is substantially reduced, well below the observational limit of 2 solar masses. This poses a serious problem for the microscopic theory of NS interior. A way out of this puzzle was proposed in ref. [36], where it was proposed that an additional repulsion in all channels, both in the nucleonic and hyperonic sectors, can be provided by the process of multi-pomeron exchange. The pomeron has the quantum number of the vacuum, and as such the process acts universally in all channels. The problem was overcome also in the calculations of ref. [37], where the DBHF method was extended to the hyperonic sector assuming SU(6) symmetry, which is mainly equivalent to the introduction of a three-body force which acts in analogous way in the nucleonic and hyperonic sectors. Both approaches show that the observational limit of the NS masses can be reached only if one assumes a TBF in the hyperonic sector at least as strong as in the nucleonic sector. These solutions of the puzzle rely on specific models for the strange sector interaction, and they could be justified only by more microscopic approaches.

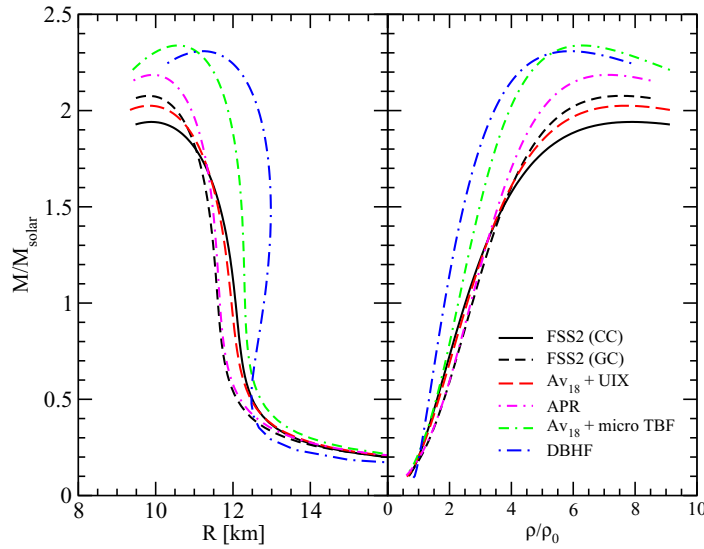


**Figure 11.** Neutron Star mass as a function of radius (left panel) and as a function of central density (right panel) for different microscopic EoS. Figure taken from [28].

Finally one should also consider the possibility of the appearance of quark matter in the NS core. Also in this case one usually finds that the EoS for NS matter becomes softer, and it is again quite uncertain if the observational limit can be reached. This is especially true if the simple bag model is used for the quark matter EoS. A discussion on this point can be found in ref. [38], where an alternative approach is presented based on the Nambu-Jona Lasinio model with the addition of a vector and di-quark interaction. With a suitable choice of the parameters it is indeed possible to overcome the observational limit. A microscopic approach to this problem based on QCD is still lacking. It would be challenging to try the extension of the QM interaction, devised for the nucleonic matter, to the region of deconfined quark matter.

#### 4. Conclusions

It has been shown that a NN interaction based on quark degree of freedom [25, 28] can be performing at least at the same level as the best NN interaction based on meson exchange processes or on the chiral symmetry of QCD. In addition, without the introduction of TBF or parameters other than the ones introduced in the fitting of the NN phase shifts and deuteron properties, the interaction is able to reproduce the three-body properties, also in the continuum, and at the same time the saturation point of nuclear matter. The latter result can be obtained only by including in the many-body calculation the three-body correlations within the hole-line expansion of the BBG formalism. These results seem to indicate that the explicit introduction of the quark structure of the nucleons is of decisive relevance for the NN interaction, in particular the effect of the TBF processes, introduced in the more traditional interactions, are to a large extent automatically included. In the physics of NS one has to explore the possible appearance of hyperons and eventually deconfined quark matter in the star core. Furthermore it would be desirable to consider other interactions based on quark degrees of freedom in order to understand if the properties of the considered interaction is a common feature of this type of interactions, and eventually to pin down the main reasons of their high performances. All that is left to future works.

## Acknowledgments

The author wishes to acknowledge the “NewCompStar” COST Action MP1304.

## References

- [1] For a brief review see Baldo M and Burgio G F 2012 *Rep. Prog. Phys.* **75** 026301
- [2] Wiringa R B, Stoks V G J and R. Schiavilla 1995 *Phys. Rev. C* **51** 38
- [3] Baldo M and Maieron C 2007 *J. Phys. G :Nucl. Part. Phys.* **34** R1
- [4] Grangé P, Lejeune A, Martzolff M and Mathiot J-F 1989 *Phys. Rev. C* **40** 1040; Zuo W, Lejeune A, Lombardo U and Mathiot J-F 2002 *Nucl. Phys. A* **706** 418; 2002 *Eur. Phys. J. A* **14** 469
- [5] Baldo M, Robledo L M, Schuck P and Viñas X 2013 *Phys. Rev. C* **87** 064305
- [6] Machleidt R 1989 *Adv. Nucl. Phys.* **19** 189
- [7] Brown G E, Weise W, Baym G and Speth J 1987 *Comm. Nucl. Part. Phys.* **17** 39
- [8] Akmal A, Pandharipande V R and Ravenhall D G 1989 *Phys. Rev. C* **58** 1804
- [9] Weinberg S 1990 *Phys. Lett. B* **251** 288; 1991 *Nucl. Phys. B* **363** 3; 1992 *Phys. Lett. B* **295** 114; 1968 *Phys. Rev.* **166** 1568
- [10] Hebeler K, Bogner S K, Furnstahl R J, Nogga A and Schwenk A 2011 *Phys. Rev. C* **83** 031301
- [11] Sammaruca F, Coraggio L, Holt JW, Itaco N, Machleidt R and Marcucci L E 2015 *Phys. Rev. C* **91** 054311
- [12] Hagen G, Papenbrock T, Ekström A, Wendt K A, Baardsen G, Gandolfi S, Hjorth-Jensen M and Horowitz CJ 2014 *Phys. Rev. C* **89** 014319
- [13] Logoteta D, Bombaci I and Kievsky A 2016 *Phys. Lett. B* **758** 449
- [14] Oka M and Yazaki K 1980 *Phys. Lett. B* **90** 41; 1981 *Prog. Theor. Phys.* **66** 556; 1981 *Prog. Theor. Phys.* **66** 572; in *Quarks and Nuclei*, edited by W. Weise (World Scientific, Singapore, 1984), p. 489.
- [15] Wong C W 1986 *Phys. Rep.* **136**, 1
- [16] Oka M, Shimizu K and Yazaki M 1987 *Nucl. Phys. A* **464** 700
- [17] Shimizu K 1989 *Rep. Prog. Phys.* **52** 1
- [18] Shimizu K, Takeuchi S and Buchmann A J 200 *Prog. Theor. Phys. Suppl.* **137** 43
- [19] Valcarce A, Garcilazo H, Fernández F and González P 2005 *Rep. Prog. Phys.* **68** 965
- [20] Fujiwara Y, Suzuki Y and Nakamoto C 2007 *Prog. Part. Nucl. Phys.* **58** 439
- [21] Fujiwara Y, Fujita T, Kohno M, Nakamoto C and Suzuki Y 2001 *Phys. Rev. C* **65** 014002
- [22] Fujiwara Y, Suzuki Y, Kohno M and Miyagawa K 2008 *Phys. Rev. C* **77** 027001
- [23] Fujiwara Y and Fukukawa K 2013 *Few-Body Systems* **54** 2357
- [24] Fujiwara Y 2014 *Few-Body Syst.* **55** 993
- [25] Baldo M and Fukukawa K 2014 *Phys. Rev. Lett.* **113** 242501
- [26] Dutra M, Laureño O, Sá Martins J S, Delfino A, Stone J R and Stevenson P D 2012 *Phys. Rev. C* **85** 035201
- [27] Baldo M and Burgio G F 2016 *Progress in Particle and Nuclear Physics* **91** 203
- [28] Fukukawa K, Baldo M, Burgio G F, Lo Monaco L and Schulze H-J 2015 *Phys. Rev.* **92**, 065802 (2015)
- [29] Gross-Boelting T, Fuchs C and Faessler A 1999 *Nucl. Phys. A* **648** 105
- [30] Danielewicz P, Lacey R and Lynch W 2002 *Science* **298** 1592
- [31] Miskowiec D *et al.* 1994 *Phys. Rev. Lett.* **72** 3650
- [32] Danielewicz P and Lee J 2014 *Nucl. Phys. A* **922**, 1
- [33] Benhar O and Valli M 2007 *Phys. Rev. Lett.* **99** 232501
- [34] *Compressed Baryonic Matter in Laboratory Experiments*, Friman B, Höhne C, Knoll J, Leupold S, Randrup J, Rapp R and Senger P (editors) 2011 *Lecture Notes in Physics Vol. 814* Springer
- [35] Antoniadis J *et al.* 2013 *Science* **340** 1233232
- [36] Yamamoto Y, Furumoto T, Yasutake N and Rijken Th A 2014 *Phys. Rev. C* **90** 045805
- [37] Katayama T and Saito K 2015 *Phys. Lett. B* **747** 43
- [38] Koyo T, Powell P D, Song Y and Baym G 2015 *Phys. Rev. D* **91** 045003